Chinese Chemical Letters 37 (2026) 111280

Contents lists available at ScienceDirect

Chinese Chemical Letters

journal homepage: www.elsevier.com/locate/cclet

Nitrogen-doped Sierpiński triangle fractals: From model to reality

Huamei Chen[a,1], Damian Nieckarz[b,1], Krisztián Palotás[c,d], Jie Li[a], Zhen Xu[a], Yajie Zhang[a,*], Marek Stankevič[e], Yang He[f,*], Kai Wu[g], Yongfeng Wang[a,*], Paweł Szabelski[b,*]

[a] Center for Carbon-based Electronics and Key Laboratory for the Physics and Chemistry of Nanodevices, School of Electronics, Peking University, Beijing 100871, China
[b] Department of Theoretical Chemistry, Institute of Chemical Sciences, Faculty of Chemistry, Maria Curie-Skłodowska University in Lublin, Pl. M.C. Skłodowskiej 3, 20-031, Lublin, Poland
[c] Institute for Solid State Physics and Optics, HUN-REN Wigner Research Center for Physics, H-1121, Budapest, Hungary
[d] HUN-REN-SZTE Reaction Kinetics and Surface Chemistry Research Group, University of Szeged, H-6720, Szeged, Hungary
[e] Department of Organic Chemistry and Crystallochemistry, Faculty of Chemistry, Institute of Chemistry Sciences, Maria Curie-Skłodowska University, Gliniana 33, 20-614, Lublin, Poland
[f] School of Material and New Energy, South China Normal University, Shanwei 516600, China
[g] BNLMS, College of Chemistry and Molecular Engineering, Peking University, Beijing 100871, China

ARTICLE INFO

Article history:
Received 5 March 2025
Revised 24 April 2025
Accepted 30 April 2025
Available online 30 April 2025

Keywords:
Sierpiński triangle fractals
Nitrogen doping
Conformationally flexible molecules
Density functional theory calculations
Monte Carlo simulation
Scanning tunneling microscopy

ABSTRACT

The Sierpiński triangle (ST) is a widely-known deterministic fractal structure that has attracted considerable attention recently. The fabrication of nitrogen-doped defect-free STs is appealing yet challenging. This is due to factors such as the increase in active sites, the random generation of nucleation centers, and the experimental growth conditions. In this contribution, we utilize a combination of density functional theory (DFT), Monte Carlo simulation (MC) and scanning tunneling microscopy (STM) to investigate the formation of nitrogen-doped STs. These STs are formed with nitrogen-rich, conformationally flexible 2,2′:6′,2″-terpyridine-6,6″-dicarbonitrile (TDBT) molecules and Fe atoms on Au(111). The replacement of benzenes with three pyridine side groups facilitates the formation of the nitrogen-doped STs with a relatively high order because of the energetic preference of molecular configurations. The introduction of the rigid 4,4″-dicyano-1,1′:3′,1″-terphenyl (C3PC) molecules markedly induces the structural transformation of the STs from ordered to high-entropy. Moreover, the nitrogen-doped STs with an order of up to 4 can be directly visualized by low-temperature STM.

© 2026 Published by Elsevier B.V. on behalf of Chinese Chemical Society and Institute of Materia Medica, Chinese Academy of Medical Sciences.

The Sierpiński triangle (ST), a captivating fractal structure renowned for its self-similarity and non-integer dimensional space-filling properties, has long fascinated researchers due to its elegance and structural beauty [1–14]. Since its theoretical prediction [15,16], significant progress has been made in assembling defect-free STs on single-crystalline surfaces using various molecular precursors through intermolecular interactions, including halogen bonds [1], hydrogen bonds [4,13], coordination bonds [2,5,10], covalent bonds [7–9] and electrostatic interaction [11]. Notably, the order of molecular STs has recently reached an impressive level of 5 through advanced templating and coassembly techniques [5]. These aperiodic yet highly ordered structures exhibit remarkable mechanical, optical, electronic, and magnetic properties [17–22], making them promising candidates for next-generation electronic devices [23].

In order to apply STs to future application, it is essential to tailor their electronic and magnetic characteristics. Nitrogen doping emerges as a powerful strategy to engineer these characteristics in nanomaterials through mechanisms, such as band structure engineering, spin polarization effects, multi-scale charge redistribution, and topological enhancement [24–26]. The synergistic interplay between fractal geometry and nitrogen doping will create unique opportunities for designing quantum materials with programmable electronic and magnetic landscapes. However, it is a formidable challenge. The increased number of active sites, the stochastic nature of nucleation center formation, and the variability in experimental growth conditions all contribute to the complexity of this process [1,7,27,28]. To address these challenges, we present a groundbreaking approach that combines density functional theory (DFT) calculations and coarse-grained Monte Carlo (MC) simulations with scanning tunneling microscopy (STM) to investigate the formation of nitrogen-doped ST fractals.

* Corresponding authors.
E-mail addresses: yjzhang11@pku.edu.cn (Y. Zhang), heyang@m.scnu.edu.cn (Y. He), yongfengwang@pku.edu.cn (Y. Wang), pawel.szabelski@mail.umcs.pl (P. Szabelski).
[1] These authors contributed equally to this work.

https://doi.org/10.1016/j.cclet.2025.111280
1001-8417/© 2026 Published by Elsevier B.V. on behalf of Chinese Chemical Society and Institute of Materia Medica, Chinese Academy of Medical Sciences.

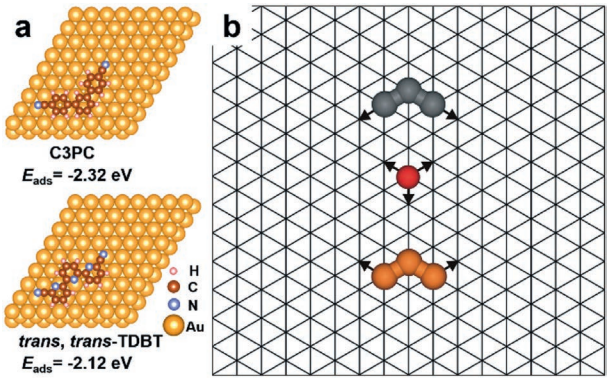


Fig. 1. (a) DFT-calculated adsorption energies of C3PC and *trans, trans*-TDBT at fcc site of Au(111) equal to -2.32 eV and -2.12 eV, respectively. (b) The corresponding coarse-grained models used in the Monte Carlo computer simulations on a flat triangular lattice. The black arrows next to the molecules indicate the bonding positions of carbonitrile functional groups that provide ligand → metal coordination bonds. The black arrows pointing outward the Fe atom (red circle) show the attachment sites available to the ligand molecules.

Our strategy leverages nitrogen-rich, conformationally flexible 2,2′:6′,2″-terpyridine-6,6″-dicarbonitrile (TDBT) molecules and Fe atoms on an Au(111) surface. By replacing benzene groups with pyridine moieties, we achieve a thermodynamically favorable molecular configuration, enabling the formation of high-order, defect-free nitrogen-doped STs. Furthermore, the introduction of rigid 4,4″-dicyano-1,1′:3′,1″-terphenyl (C3PC) molecules induces a structural transformation from ordered to high-entropy states, offering new insights into the design of ST heterostructures. By directly visualizing nitrogen-doped STs with orders up to 4 using low-temperature STM, we demonstrate the practical feasibility of our approach. This study not only advances our understanding of nitrogen-doped STs but also establishes a robust framework for doping other elements into molecular ST systems.

TDBT is a conformationally flexible molecule functionalized with terpyridine group and two carbonitrile end groups, allowing for easy chemical and structural tuning. And it is successfully obtained *via* one-step organic synthesis (Figs. S1-S4 in Supporting information). Based on the orientation of outermost bipyridyl moieties in the TDBT backbone, TDBT adopts either *cis*- or *trans*-configurations, labelled as *trans, trans*-, *cis, cis*-, *trans, cis*$_L$- and *trans, cis*$_R$-TDBT (Fig. S5 in Supporting information). To understand the adsorption behavior of TDBT, we performed the corresponding DFT calculations using a single molecule with the end pyridine ring centered at the fcc, hcp and top sites of Au(111). Moreover, two molecular orientations, one rotated by 30° with respect to the other (0°), were considered for adsorption site of each type. As indicated by the theoretical calculations, the *trans, trans*-TDBT configuration adsorbed at fcc site of Au(111) surface is the energetically most favorable structural motif among all the conformers (Figs. S6-S10 in Supporting information). The same favored fcc adsorption position is found for rigid 4,4″-dicyano-1,1′:3′,1″-terphenyl (C3PC) molecule, which has been widely used to build STs *via* coordination bonding [2,3,5,20] and hydrogen bonding [4,13], respectively. The C3PC is more stable with an adsorption energy of -2.32 eV in comparison to TDBT with -2.12 eV (Fig. 1a). The adsorption energy (E_{ads}) is defined as, $E_{ads} = E_{(substrate+molecule)} - E_{(substrate)} - E_{(molecule)}$, where $E_{(substrate+molecule)}$, $E_{(substrate)}$ and $E_{(molecule)}$ refers to the energy of the molecule on the substrate, the substrate and the molecule in vacuum, respectively.

To understand the formation of nitrogen-doped STs, we applied a simplified coarse-grained model based on our prior results regarding the fractal structure formation in surface-confined metal-organic assemblies [15,16]. Considering the energetically most favorable adsorbed configurations obtained with the DFT method, the model TDBT and C3PC units were designed in a way to reflect the corresponding optimal molecular conformations. Specifically, the molecules of TDBT and C3PC were modeled as rigid, rod-like structures with a 120° bend, each comprising three interconnected segments. For TDBT, each segment represents a single pyridyl ring. These tectons were designed to have centers for directional interactions, which were positioned so as to correspond with the locations of the carbonitrile groups in each tecton. The Au(111) crystalline substrate surface was modeled as a triangular lattice of equivalent adsorption sites, characterized by a lattice constant $\alpha = 1$. It was assumed that the inter-segment-center distance in both TDBT and C3PC equals a, allowing each molecular segment to occupy a single adsorption site. Fe atoms were represented as single segments, and followed the same one-to-one restriction when occupying adsorption sites. Three interaction directions were assigned to the Fe atoms, with each pair forming an angle of 120°. An attractive interaction between a tecton and a metal atom was effective only when these components occupied adjacent sites and when their corresponding interaction directions were collinear (*i.e.*, aligned →←), with each →← interaction contributing $\varepsilon = -1$. The comprehensive explanation of the above is illustrated in Fig. 1b. Moreover, it was assumed that the energy of different metal-linker nodes depends solely on the number of attached molecules and not on their nodal configuration. Fig. S12 (Supporting information) illustrates the coordination bonding rules applied in the model, along with the resulting nodal motifs and their corresponding energies. A detailed description of the simulation procedure and model parameters is provided in Section 3 (Supporting information).

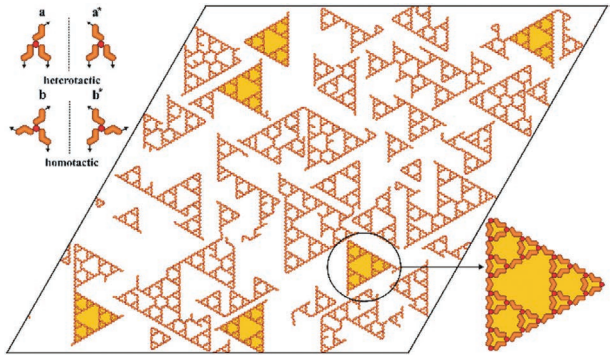


Fig. 2. Snapshot of the adsorbed overlayer comprising 1800 *trans, trans*-TDBT molecules and 1200 Fe adatoms taken at temperature $T = 0.001$. The magnified heterotactic and homotactic coordination nodes are presented in the top-left insets, respectively. A defect-free achiral ST-3 fractal aggregate is magnified in the bottom-right inset.

To explore the nitrogen-doped fractal self-assembly, we first performed the MC simulations for a metal-organic overlayer composed of 1800 *trans, trans*-TDBT molecules (orange sticks) and 1200 Fe atoms (red circles) with a stoichiometric ratio 3:2, which was optimal for the development of extended self-similar structures [16]. As shown in the middle of Fig. 2, the adsorbed components self-assembled into a whole series of fractal aggregates with special aperiodicity and ordered topography. Among them, the largest structure in the overlayer can be considered as a realization of the third-order Sierpiński triangle (magnified in bottom-right inset). In such a structure, there are 9 smaller triangles, each comprising 3 Fe atoms. Moreover, 27 Fe atoms are linked by 39 *trans, trans*-TDBT molecules. For the 120° V-shaped precursors, there are two types of node conformation, *i.e.*, heterotactic and homotactic nodes. Only heterotactic nodes are responsible for the growth of STs with the correct geometry. For the heterotactic nodes, two forms, here denoted arbitrarily as a and a*, can be present as mirror images of each other (see nodes in the top-left inset). The calculated binding energy of Fe-(*trans, trans*-TDBT)$_3$ complex by DFT is around -3.93

eV (Fig. S11 in Supporting information). However, the equal probability of a and a* leads to STs with racemic composition in both the simulation and experiment, like in C3PC-STs systems [2,3]. Statistically, the homotactic nodes accounted for 7.1% of the three-fold nodes (Table S1 in Supporting information) in the modeled system, and they were the source of structural errors and detrimental to the further growth of STs. The heterotactic nodes dominate the adsorbed phase due to the greater number of ways a node of this type can be formed from a two-fold node by attaching an additional molecule (Fig. S12). The Fe atoms effectively support these heterotactic motifs, especially at low temperatures at which thermal energy is not sufficient to break the (increasingly stronger) metal-linker bonds (Fig. S13 in Supporting information). This effect is even more significant in the case of the release of a metal atom from the three-fold node, which would require breaking three bonds. As a result, the directional metal-linker interactions imposed by the three-coordinate 120° Fe centers govern the self-assembly of the STs.

The potentially effective way to enhance the quality of STs was to reduce the number of homotactic nodes (Fig. S14 in Supporting information), for example, through the synergistic effect of intermolecular and molecule-substrate interactions and the regulation of the thermodynamic equilibrium in the experiments [1,7,8]. Another factor impeding the fractal aggregates was their growth mechanism. Unlike the normal Ostwald ripening, the number of active sites that attach molecules or atoms at three accessible vertices does not increase with the perimeter of the triangle but remains constant all the time. As a result, it is more difficult to attach the subsequent molecule in bigger triangles. Consequently, a collection of relatively small aggregates has been frequently obtained in both experiments and MC computer simulations.

Fig. 3 presents the results obtained for 900 *trans, trans*-TDBT molecules (orange sticks) and 900 C3PC molecules (gray sticks) coadsorbed with 1200 Fe atoms (red circles) in 3:3:4 ratio. In comparison with the monomolecular TDBT fractal structure (Fig. 2), the introduction of C3PC molecules significantly diminishes the degree of orderliness of the heterogeneous nitrogen-doped fractal structure. In fact, the number of possible nodal motifs increased from 4 to 16 (Fig. 3b). Each node was formed of homomolecular (3 C3PC or 3 *trans, trans*-TDBT) or heteromolecular (2 C3PC + *trans, trans*-TDBT or C3PC + 2 *trans, trans*-TDBT) composition. Among them, only eight types of heterotactic nodes can attach another molecule (C3PC or *trans, trans*-TDBT) to form closed triangles for larger STs. The homotactic nodes prevented fractals from growing larger and were accountable for the formation of erroneous structures. Interestingly, both individual C3PC-Fe-ST-n and *trans, trans*-TDBT-Fe-ST-n (n represents the order of the STs, and varies between 0 and 4 in this work) have never been observed in the theoretically studied systems. It implied that the entropy of mixing played a significant role in directing the assembly of three components. The above descriptions suggest that nitrogen-doped self-similar architectures can be predicted *ab initio* by means of the simplified coarse-grained approach.

To demonstrate the accurate predictive capabilities of the model proposed in this work, we conducted the relevant STM experiments on the Au(111) surface under ultra-high vacuum (UHV) conditions. The corresponding results are shown in Figs. 4 and 5. In the experiments, the *trans, trans*-TDBT dominated in molecular assemblies (Fig. S15 in Supporting information), which highlighted the energetic preference of the molecular bipyridine fragment on Au(111). This is in good agreement with the DFT-calculated results shown in Figs. S6-S10. This delicate free-energy bias of TDBT configurations results in the growth of nitrogen-doped STs in simulations and experiments.

After thermally sublimating Fe atoms onto a *trans, trans*-TDBT-precovered Au(111) surface held at 200 K, a mixture of different

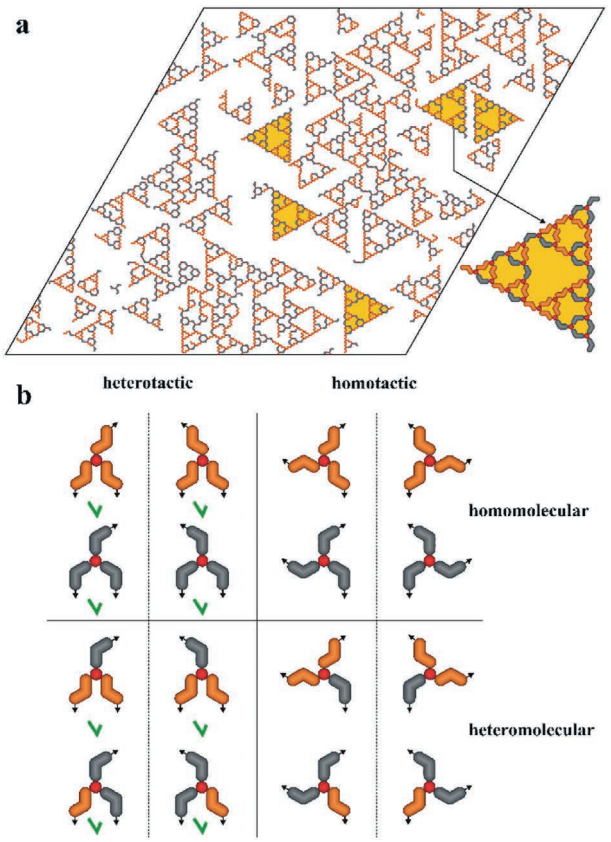


Fig. 3. (a) Snapshot of the simulated system comprising 900 *trans, trans*-TDBT molecules (orange sticks), 900 C3PC molecules (gray sticks) and 1200 Fe atoms (red circles) taken at temperature $T = 0.001$. The defect-free mixed ST-3 fractal aggregates are marked in deep yellow color, one of which is magnified in the right inset. (b) Survey of 16 possible three-fold coordination nodes (containing homomolecular and heteromolecular composition), and the dashed line represents the mirror plane. The green checks in the left plane indicate nodes that could form STs.

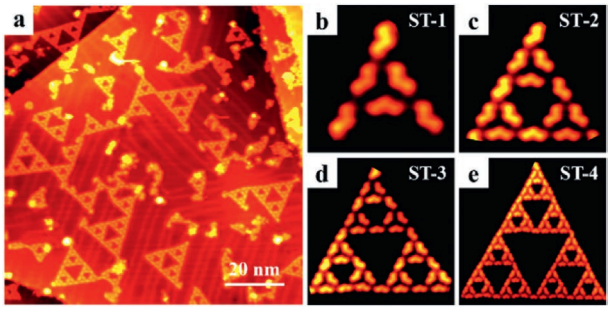


Fig. 4. STM images of *trans, trans*-TDBT-Fe-ST-n with n equals 1, 2, 3, 4, respectively. Imaging conditions: (a) $V_{bias} = -1000$ mV, $I_t = 20$ pA; (b) $V_{bias} = 10$ mV, $I_t = 100$ pA; (c) $V_{bias} = 10$ mV, $I_t = 100$ pA; (d) $V_{bias} = 30$ mV, $I_t = 100$ pA; (e) $V_{bias} = -300$ mV, $I_t = 100$ pA.

generations of nitrogen-doped metal organic STs can be formed at a relatively low coverage (~0.5 ML). These STs have markedly different morphologies from the self-assembly of the *trans, trans*-TDBT molecule (Fig. S15), thus confirming formation of coordination bonds between -CN and Fe atoms. From the large-scale images, we observed that the Au(111) surface was covered by nitrogen-doped STs (Fig. 4a). The details of the successive generations of ST-n are presented in Figs. 4b-e. The geometric fidelity of STs is fundamentally governed by the conformational properties of their elementary motifs. Two distinct nodal configurations emerge upon Fe coordination: heterotactic and homotactic nodes (Fig. S16 in Supporting information). STs are exclusively composed of het-

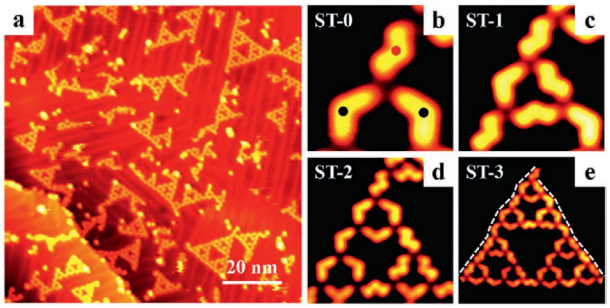


Fig. 5. STM images of C3PC-*trans, trans*-TDBT-Fe-ST-n with n equals 0, 1, 2, 3, respectively. Imaging conditions: (a) V_{bias} = -1000 mV, I_t = 20 pA; (b) V_{bias} = -100 mV, I_t = 20 pA; (c) V_{bias} = -100 mV, I_t = 20 pA; (d) V_{bias} = -100 mV, I_t = 20 pA; (e) V_{bias} = -500 mV, I_t = 15 pA. The C3PC and *trans, trans*-TDBT molecules are marked by black and red circles, respectively.

erotactic nodes at every vertex. The formation of homotactic nodes acted as a defect and was harmful to further ST growth. However, it was also experimentally unavoidable. As the two kinds of nodes are energetically equivalent, the formation of the STs originates mainly from the entropic stabilization of the heterotactic nodes which have a larger number of in-plane orientations compared to the homotactic nodes; 6 *vs*. 2, respectively [16]. The remarkable stability of STs is mainly attributed to the synergistic effect of intermolecular interactions (-CN-Fe) and adsorbate-substrate interactions. From the topological point of view, the V-shaped *trans, trans*-TDBT molecules with openings pointing outward led to a smaller pore of ST-1 than that comprised of rigid C3PC molecules. The total number of empty voids ranged from 0 to 40, with these two values corresponding to ST-0 and ST-4, respectively. In an ST-n, the numbers of Fe atoms and *trans, trans*-TDBT were determined as 3^n and $(3^{n+1}+3)/2$, respectively. For example, in ST-0 and ST-4, there are 1 and 81 Fe atoms, and 3 and 123 *trans, trans*-TDBT molecules, respectively.

After introducing C3PC into *trans, trans*-TDBT-Fe ST, a whole series of mixed, disordered C3PC-*trans, trans*-TDBT-Fe-ST-n spontaneously formed. Experimentally, we have not observed any mutually independently existing of C3PC-Fe-ST-n and *trans, trans*-TDBT-Fe-ST-n fragments, and this was in good accordance with the MC simulation (Fig. 3). There are two ways to experimentally distinguish C3PC from *trans, trans*-TDBT molecules. First, depending on the position of -CN on the molecular backbone, C3PC molecules appear longer than *trans, trans*-TDBT molecules. Fig. 5b presents a high-resolution STM image of a ST-1, with one small *trans, trans*-TDBT and two large C3PC being marked by red and black circles respectively. When some *trans, trans*-TDBT molecules in the *trans, trans*-TDBT-Fe-ST-n system were replaced by C3PC molecules, the other TDBT molecules were required to change their positions relative to the Fe atoms. This might lead to wavy edges and heterologous triangular pores of C3PC-*trans, trans*-TDBT-Fe-ST-n (Fig. 5e). Such heterologous pores may function as molecular sieves, which are capable of selectively capturing or immobilization of guest molecules of different sizes.

In summary, this study successfully demonstrates the construction of nitrogen-doped STs through an integrated approach combining coarse-grained Monte Carlo simulations, DFT calculations and STM fabrication and characterization. The strategic substitution of benzene groups with pyridine moieties significantly facilitates the formation of defect-free nitrogen-doped ST systems, primarily attributed to the thermodynamic preference for stable molecular configurations. Furthermore, the incorporation of rigid 4,4″-dicyano-1,1′:3′,1″-terphenyl (CP3C) molecular building blocks enables the fabrication of ST heterostructures. These findings establish a robust methodology for doping other elements in molecular ST systems and potentially promote the development of advanced functional materials with tailored electronic and magnetic characteristics.

Declaration of competing interest

The authors declare that they have no known competing financial interests or personal relationships that could have appeared to influence the work reported in this paper.

CRediT authorship contribution statement

Huamei Chen: Writing – review & editing, Writing – original draft, Formal analysis, Data curation. **Damian Nieckarz:** Writing – review & editing, Writing – original draft, Methodology, Formal analysis, Data curation. **Krisztián Palotás:** Writing – review & editing, Funding acquisition, Data curation. **Jie Li:** Writing – review & editing, Data curation. **Zhen Xu:** Writing – review & editing. **Yajie Zhang:** Writing – review & editing, Supervision, Data curation. **Marek Stankevič:** Writing – review & editing. **Yang He:** Writing – review & editing, Supervision, Data curation. **Kai Wu:** Writing – review & editing. **Yongfeng Wang:** Writing – review & editing, Supervision, Project administration, Funding acquisition, Conceptualization. **Paweł Szabelski:** Writing – review & editing, Supervision, Funding acquisition, Data curation.

Acknowledgments

This work is supported by the National Science Centre, Poland, Project (Nos. 2018/31/D/ST4/01443, SONATA 14), National Natural Science Foundation of China (Nos. 22225202, 92356309, 22132007, 21991132, 22172002), National Research Development and Innovation Office of Hungary (No. K138714). Experiments are supported by Peking Nanofab. DFT calculations were carried out on the HUN-REN Hungarian Research Network.

Supplementary materials

Supplementary material associated with this article can be found, in the online version, at doi:10.1016/j.cclet.2025.111280.

References

[1] J. Shang, Y. Wang, M. Chen, et al., Nat. Chem. 7 (2015) 389–393.
[2] Q. Sun, L. Cai, H. Ma, et al., Chem. Commun. 51 (2015) 14164–14166.
[3] N. Li, X. Zhang, G. Gu, et al., Chin. Chem. Lett. 26 (2015) 1198–1202.
[4] X. Zhang, N. Li, G. Gu, et al., ACS Nano 9 (2015) 11909–11915.
[5] C. Li, X. Zhang, N. Li, et al., J. Am. Chem. Soc. 139 (2017) 13749–13753.
[6] Y. Wang, N. Xue, R. Li, et al., ChemPhysChem 20 (2019) 2262–2270.
[7] Y. Mo, T. Chen, J. Dai, et al., J. Am. Chem. Soc. 141 (2019) 11378–11382.
[8] G. Feng, Y. Shen, Y. Yu, et al., Chem. Commun. 57 (2021) 2065–2068.
[9] G. Gu, N. Li, L. Liu, et al., RSC Adv. 6 (2016) 66548–66552.
[10] S. Li, R. Zhang, L. Kang, et al., ACS Nano 15 (2021) 18014–18022.
[11] J. Dai, X. Zhao, Z. Peng, et al., J. Am. Chem. Soc. 145 (2023) 13531–13536.
[12] X. Li, Z. Xu, D. Bu, et al., Chin. Chem. Lett. 35 (2024) 110055.
[13] C. Li, R. Li, Z. Xu, et al., J. Am. Chem. Soc. 143 (2021) 14417–14421.
[14] X. Zhang, R. Li, N. Li, et al., Chin. Chem. Lett. 29 (2018) 967–969.
[15] D. Nieckarz, P. Szabelski, J. Phys. Chem. C 117 (2013) 11229–11241.
[16] D. Nieckarz, P. Szabelski, Chem. Commun. 50 (2014) 6843–6845.
[17] A. Wang, M. Zhao, Phys. Chem. Chem. Phys. 17 (2015) 21837–21844.
[18] E. van Veen, S. Yuan, M.I. Katsnelson, et al., Phys. Rev. B 93 (2016) 115428.
[19] H. Wang, X. Zhang, Z. Jiang, et al., Phys. Rev. B 97 (2018) 115451.
[20] R. Li, N. Xue, X. Zhang, et al., J. Phys. Chem. C 125 (2021) 5581–5586.
[21] D. Wang, L. Dong, G. Gu, Adv. Funct. Mater. 33 (2023) 2208849.
[22] F. De Nicola, N.S.P. Purayil, D. Spirito, et al., ACS Photonics 5 (2018) 2418–2425.
[23] X. Li, Z. Xu, D. Bu, et al., Chin. Chem. Lett. 36 (2025) 110100.
[24] L. Conrad, J.S. Sturm, I. Alcón, et al., J. Phys. Chem. C 128 (2024) 18886–18893.
[25] K. Sun, N. Cao, O.J. Silveira, et al., Sci. Adv. 11 (2025) eads1641.
[26] E.C.H. Wen, P.H. Jacobse, J. Jiang, et al., J. Am. Chem. Soc. 145 (2023) 19338–19346.
[27] T. Lin, X. Shang, J. Adisoejoso, et al., J. Am. Chem. Soc. 135 (2013) 3576–3582.
[28] P.B. Weber, R. Hellwig, T. Paintner, et al., Angew. Chem. Int. Ed. 55 (2016) 5754–5759.